Controlled Frustration Release on the Kagome Lattice by Uniaxial-Strain Tuning

Jierong Wang,[1] M. Spitaler,[2] Y.-S. Su,[1] K. M. Zoch,[3] C. Krellner,[3]
P. Puphal,[3,4] S. E. Brown,[1] and A. Pustogow[1,2,*]

[1]*Department of Physics and Astronomy, UCLA, Los Angeles, California 90095, USA*
[2]*Institute of Solid State Physics, TU Wien, 1040 Vienna, Austria*
[3]*Institute of Physics, Goethe-University Frankfurt, 60438 Frankfurt (Main), Germany*
[4]*Max-Planck-Institute for Solid State Research, 70569 Stuttgart, Germany*

It is predicted that strongly interacting spins on a frustrated lattice may lead to a quantum disordered ground state or even form a quantum spin liquid with exotic low-energy excitations. However, a controlled tuning of the frustration strength, separating its effects from those of disorder and other factors, is pending. Here, we perform comprehensive ^{1}H NMR measurements on $Y_3Cu_9(OH)_{19}Cl_8$ single crystals revealing an unusual $\vec{Q} = (1/3 \times 1/3)$ antiferromagnetic state below $T_N = 2.2$ K. By applying *in situ* uniaxial stress, we break the symmetry of this disorder-free, frustrated kagome system in a controlled manner yielding a linear increase of T_N with strain, in line with theoretical predictions for a distorted kagome lattice. In-plane strain of $\approx 1\%$ triggers a sizable enhancement $\Delta T_N/T_N \approx 10\%$ due to a release of frustration, demonstrating its pivotal role for magnetic order.

DOI: 10.1103/PhysRevLett.131.256501

Even after decades of intense scrutiny, quantum spin liquids (QSLs) remain an elusive state of matter [1–4]. Apart from growing evidence for the importance of disorder [5–14], geometrical frustration is considered decisive to suppress magnetic order in the presence of strong antiferromagnetic (AFM) exchange interactions. The vast majority of QSL candidates are found in quasi-2D correlated electron systems with triangular [14–18], honeycomb [19], or kagome [20,21] lattices. Herbertsmithite, $ZnCu_3(OH)_6Cl_2$, is an archetype realization of the latter symmetry [21] and has been intensely studied over the past two decades [5,13,21–27]—not least due to the exciting proposal of exotic superconductivity and Dirac bands in a doped kagome lattice [28]. Although the latter scenario could not be realized in Ga-herbertsmithite [29], many related compounds substituting Zn by other bi- or trivalent cations have been synthesized by now [20]. Among those, $Y_3Cu_9(OH)_{19}Cl_8$ [30,31] (denoted as Y-kapellasite) and $YCu_3(OH)_6Cl_3$ [32] crystallize in the closely related kapellasite structure (see Fig. 1) and exhibit AFM order at temperatures $T_N \ll J/k_B \approx 10^2$ K.

So far, most attempts to modify the frustration strength focused on chemical substitution in order to arrange the valence electrons in the above-mentioned patterns. While commonly physical pressure is applied to tune electronic interactions, e.g., toward metal-insulator transitions, hydrostatic compression does not directly affect the lattice symmetry, unless it triggers a structural transition. Recent developments in piezoelectric uniaxial-strain applications at cryogenic temperatures [34] now provide us the opportunity to modify the degree of geometrical frustration in a controlled manner.

Here, we take full advantage of uniaxial strain to directly control magnetic order in Y-kapellasite single crystals. We characterize the magnetic properties by ^{1}H nuclear magnetic resonance (NMR) in a temperature range 1.5–200 K and reveal strong spin correlations for $T < 30$ K. Below $T_N = 2.2$ K, we find AFM order consistent with the proposed $\vec{Q} = (1/3 \times 1/3)$ state [33]. By applying uniaxial strain of the order of 1%, we directly tune the frustration of exchange interactions *in situ*, triggering a pronounced increase of T_N linear with strain.

In the two Y analogs of herbertsmithite (kapellasite), the additional charge upon substitution of Zn^{2+} is compensated
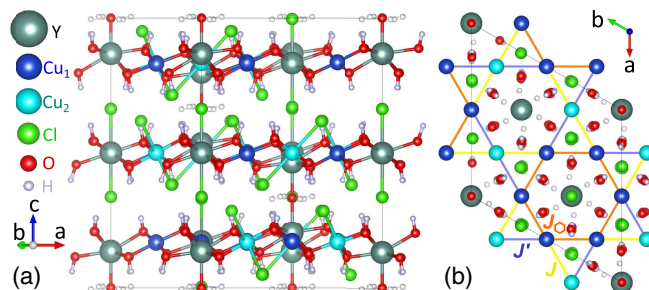

FIG. 1. Crystal structure of $Y_3Cu_9(OH)_{19}Cl_8$ (Y-kapellasite). (a) Cu^{2+} atoms (blue, cyan) arranged in layers. (b) Within the *ab* plane, they form a slightly distorted $S = 1/2$ kagome lattice that preserves threefold rotational symmetry with AFM couplings $J_\bigcirc/J \approx 1$ and $J/J' \approx 18$ [30,31,33].
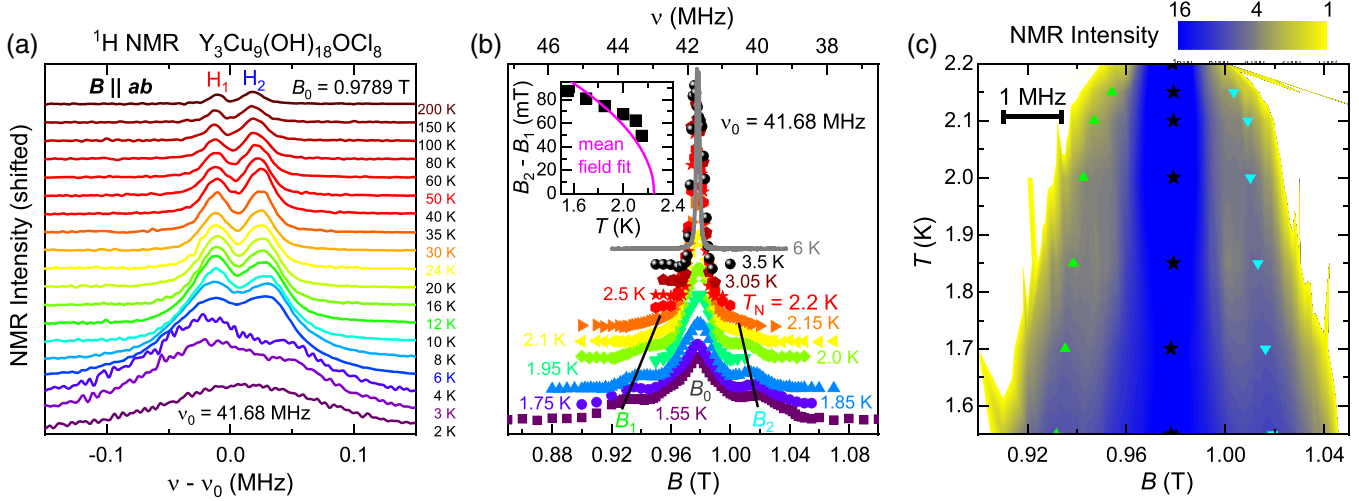
FIG. 2. (a) ^{1}H NMR spectra acquired for in-plane magnetic field ($B \perp a$, $B_0 = 0.9789$ T). At elevated temperatures, the spectra consist of two peaks (H_1 and H_2) separated by 30–40 kHz. The lines exhibit successive broadening upon cooling and exceed the experimental bandwidth below 4 K. (b) The spectra below 4 K, acquired by magnetic field sweeps at constant frequency $\nu_0 = 41.68$ MHz, reveal a pronounced splitting into three peaks below $T_N = 2.2$ K. The separation between the two outer peaks (B_1 and B_2) increases to lower T in a mean-field fashion (inset), while the central peak remains at B_0. The gray line indicates the spectrum at 6 K, which follows the frequency scale at the top. (c) The false-color plot of the data from (b) illustrates the shifting of B_1 and B_2 as well as the strong broadening. The horizontal bar corresponds to a frequency $\Delta\nu = \Delta B / {}^1\gamma = 1$ MHz.

by additional Cl and/or OH, resulting in Mott insulators with a charge-transfer gap of 3 eV ($U \approx 8$ eV [35]). In the case of YCu$_3$(OH)$_6$Cl$_3$, this leads to an unstable crystal structure—similar to GaCu$_3$(OH)$_6$Cl$_3$ [29], it can be synthesized only as powder [32,36]—while large Y$_3$Cu$_9$(OH)$_{19}$Cl$_8$ single crystals with slightly distorted kagome layers (structure shown in Fig. 1) can be grown by hydrothermal methods [30,31]. X-ray and neutron diffraction studies revealed two crystallographically inequivalent Cu sites preserving the threefold rotational symmetry of the kagome lattice [Fig. 1(b)] from 300 K down to 65 mK [30,31]. To that end, Y-kapellasite exhibits a peculiar form of frustration distinct from the isotropic lattice of ZnCu$_3$(OH)$_6$Cl$_2$. While there is strong coupling within ($J_{\bigcirc}$) and between (J) hexagons, indicated in Fig. 1(b), the weaker $J' \ll J_{\bigcirc} \approx J$ eventually stabilizes magnetic order [30,31,33]. Both Y compounds exhibit long-range AFM at $T_N \ll \Theta_{CW} \approx 100$ K; magnetization, specific heat, μSR, and neutron diffraction experiments yield $T_N = 2.2$ K for Y-kapellasite [30,31], related with the observation of terahertz magnons [37]. For YCu$_3$(OH)$_6$Cl$_3$, a broad magnetic anomaly was observed at $T_N = 15$ K [32,36,38]. Despite the apparent absence of a QSL state down to $T \to 0$, distorted kagome lattices [39–41] came into focus recently due to magnetoelastic coupling and the realization of nontrivial ground states such as pinwheel [42,43] and $\vec{Q} = (1/3 \times 1/3)$ order [33].

In our comprehensive NMR study, we first investigate the magnetic ground state of Y-kapellasite at ambient pressure. The magnetic field was aligned parallel to the

Cu^{2+} chains of the kagome network, i.e., perpendicular to the crystallographic a axis; in the following, this in-plane field configuration is denoted as $B \| ab$. Figure 2(a) presents the temperature evolution of the ^{1}H spectra ($B_0 = 0.9789$ T, $\nu_0 = 41.68$ MHz), yielding two peaks separated by 30–40 kHz above 4 K due to dipolar coupling to paramagnetic Cu^{2+} spins [44]. At lower T, the line broadening exceeds the experimental bandwidth such that an acquisition around a single frequency does not capture the entire spectrum (see Sec. I in Ref. [44]). We resolve the entire peak structure by magnetic field sweeps at constant frequency ν_0 between 1.55 and 3.5 K [Fig. 2(b)]. Below T_N, the signal splits into a triplet with the central line (B_0) remaining unshifted. The two outer peaks (B_1 and B_2) move apart with a T dependence of their separation $B_2 - B_1$ consistent with the onset of a mean-field-type broken symmetry, further illustrated by the contour plot in Fig. 2(c). On a quantitative level, the line splitting at the lowest measured temperature agrees well with a local field $B_{loc} \approx 60$–64 mT originating from dipolar coupling between ^{1}H nuclear moments and AFM ordered electron spins on the Cu^{2+} sites (see Fig. 1), which are at a distance 2.44–2.50 Å [30,31].

While our observation of a line splitting evidences AFM order setting in at T_N, the shape of the spectrum provides insight into the spin structure. Upon $\vec{Q} = (1/3 \times 1/3)$ order [Fig. 3(a)] predicted for a distorted kagome lattice with $J' \ll J_{\bigcirc} \approx J$ [33], which is realized in Y-kapellasite [see Fig. 1(b)], along a Cu^{2+} chain four successive AFM bonds are satisfied, followed by two unsatisfied bonds, as
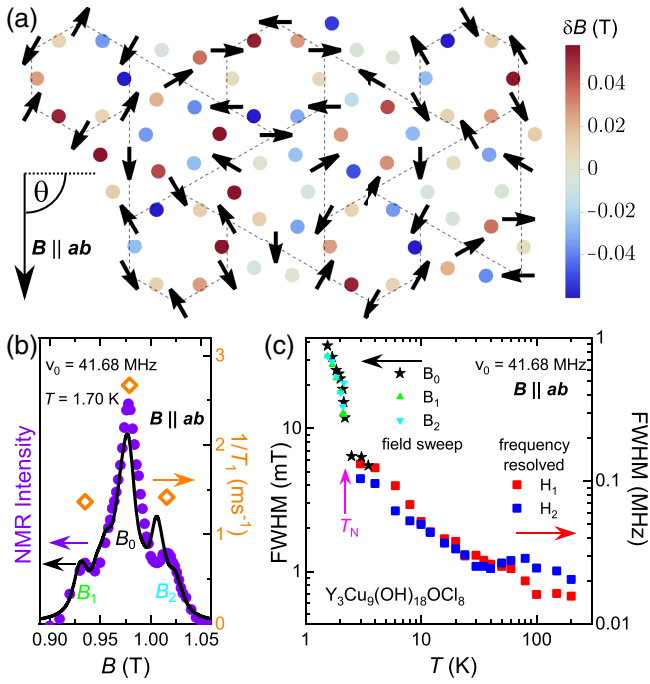
FIG. 3. (a) $Q = (1/3 \times 1/3)$ AFM order predicted for a distorted kagome lattice [33]. Colored circles indicate the location of ^{1}H nuclei in the crystal lattice of Y-kapellasite (cf. Fig. 1). The color corresponds to $\delta B = |\mathbf{B}_0 + \mathbf{B}_{loc}| - B_0$ ($B_0 = 0.9789$ T; see legend on the right). (b) The ^{1}H NMR spectrum (violet; measured at 1.70 K) consists of three main peaks B_0, B_1, and B_2 [cf. Fig. 2(b)]. The experimental data agree well with the calculated NMR spectrum (black line) upon dipolar coupling of the ^{1}H nuclei to the local magnetic field of the Cu^{2+} spins in (a). The spin-lattice relaxation rate (orange diamonds) was measured at different fields: T_1^{-1} of the side peaks (B_1 and B_2) is ≈50% smaller than for the central peak at $B_0 = 0.9789$ T. (c) The full width at half maximum (FWHM), extracted for the ^{1}H NMR peaks H_1 and H_2 [$T > T_N$; see Fig. 2(a)] as well as for the three lines B_0, B_1, and B_2 emerging below T_N [see Figs. 2(b) and 2(c)], exceeds the homogeneous linewidth below 30 K and shows a steep increase at T_N. Note the different units of the vertical scales.

visualized in Fig. 1(c) in Ref. [33]. We point out that ^{1}H nuclei are ideal probes of the local fields emerging from the Cu^{2+} spin structure, as they yield a characteristic fingerprint spectrum due to different B_{loc} at the respective sites, as sketched in Fig. 3(a). To that end, we have calculated the line shape [black solid in Fig. 3(b)] for dipolar coupling to Cu^{2+} spins upon $\vec{Q} = (1/3 \times 1/3)$ order, as described in Ref. [44]. In particular, our calculation reveals that the local field is compensated at the majority of ^{1}H sites, which corresponds to the central peak at B_0. For the red (blue) colored proton sites, $\mathbf{B}_{loc}$ adds up to (subtracts from) $\mathbf{B_0}$, yielding the satellite at B_1 (B_2). Overall, the measured ^{1}H NMR spectra are consistent with the dipolar fields upon $\vec{Q} = (1/3 \times 1/3)$ order in Y-kapellasite [33], motivating more detailed studies of this peculiar structure both at
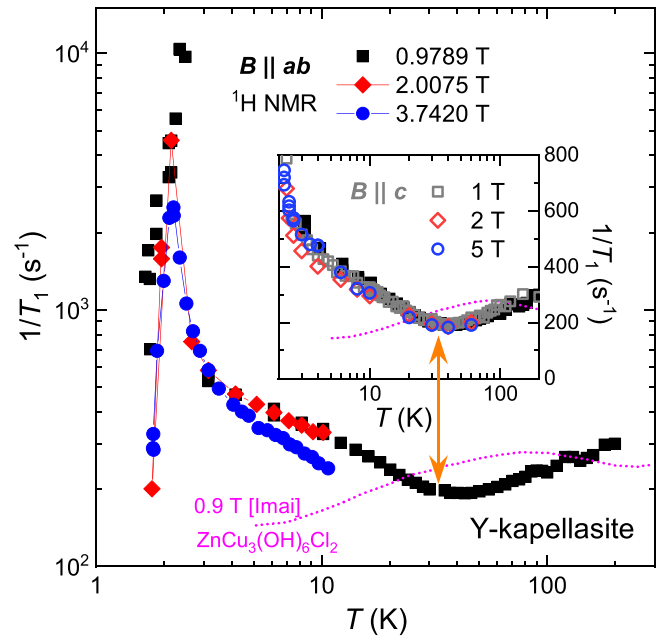
FIG. 4. The ^{1}H NMR spin-lattice relaxation rate T_1^{-1} was probed for $B\|ab$ and $B\|c$ (inset). Upon cooling from room temperature, T_1^{-1} initially decreases toward a minimum around 32 K (orange double arrow). Below that, the increase of T_1^{-1} signals the onset of strong antiferromagnetic spin fluctuations [37], which result in a sharp maximum at $T_N = 2.2$ K. Increasing the magnetic field yields a reduced peak value and broadening of the transition, consistent with specific heat results [30]. Above 4 K, T_1^{-1} does not exhibit pronounced field dependence or anisotropy. The pink dotted line indicates the ^{1}H relaxation rate of $ZnCu_3(OH)_6Cl_2$ [51].

ambient pressure and also under strain. Uniaxial distortion breaks the threefold rotational symmetry within and between the hexagons, thus changing the balance among $J_{\bigcirc}$, J, and J' [Fig. 1(b)], potentially toward a spin-liquid phase or $\vec{Q} = 0$ order [33].

Apart from the splitting, the NMR linewidth exhibits excessive broadening upon the onset of AFM [Fig. 3(c)]. The FWHM exceeds beyond the homogeneous linewidth $(\pi T_2)^{-1} \approx 35$ kHz already below $T \approx 32$ K, indicating the onset of AFM fluctuations. The spin-lattice relaxation rate T_1^{-1} is highly susceptible to the emerging magnetism below and lattice dynamics above this temperature; the minimum around 32 K in Fig. 4 lines up with a subtle structural instability reported recently [31]. Down to 4 K, we do not observe pronounced field dependence or anisotropy ($B\|c$ data in the inset in Fig. 4).

The onset of AFM order yields a sharp peak of T_1^{-1} at $T_N = 2.2$ K that decreases and slightly broadens with higher field, in accord with specific heat data [30]. Apart from measuring T_1^{-1} at $B_0 = 0.9789$ T from $T < T_N$ up to 200 K, we also probed the relaxation in the AFM state at the two outer peaks B_1 and B_2 [Fig. 3(b)]. The faster relaxation at B_0 indicates that the central peak is

more sensitive to low-energy magnons. NMR measurements at $T \ll 1$ K are highly desired in future work.

To summarize the findings so far, the NMR properties are consistent with an unusual $\vec{Q} = (1/3 \times 1/3)$ state [31,33]. T_1^{-1} is highly susceptible to the onset of AFM order and exhibits a sharp peak at T_N, making it a sensitive probe of the transition. Having identified its exotic magnetic ground state, in the following, we apply in-plane uniaxial stress to Y-kapellasite single crystals. Through compressing the kagome lattice along the Cu^{2+} chains, sketched in Fig. 5(d), we directly modify the transfer integrals t_i and, hence, the exchange interactions and their degree of geometrical frustration.

In Fig. 5, we trace the change in transition temperature upon *in situ* strain tuning by T_1^{-1} measurements at $B_0 = 1.81$ T $(B \| a)$. There is a clear enhancement of T_N with approximately linear dependence on the applied uniaxial strain $\varepsilon = (\Delta L / L)$ [inset in Fig. 5(d); Fig. 5(a) indicates the length L of the compressed part of the sample), which agrees with calculations of AFM ordering on a distorted kagome lattice [52]. Our results on two samples consistently reveal an increase of T_N by almost 10% for compressive strain of the order of 1% [53] parallel to the kagome layers. How does this compare with the modifications expected for hydrostatic pressure of similar size? For comparison, we consider that the superexchange is proportional to $t^4/(\Delta^2 U)$ and $t \propto r^{-4}$; hence, 1% reduction of Cu-Cu distance should result in an increase of 16%. Here, Δ is the charge-transfer gap, and U is the on-site Coulomb repulsion. However, this is a large overestimate, because in real materials the crystal lattice adapts mostly by changing bond angles rather than bond length [54]. Moreover, in our uniaxial-stress experiments, an increase of $J_{\bigcirc}$ and J along the direction of applied strain is likely accompanied by a decrease of comparable size in the perpendicular direction due to nonzero Poisson ratio, yielding a much smaller enhancement of the overall exchange energy. Accordingly, the sizable increase of T_N realized here by uniaxial compression goes beyond simple bandwidth tuning effects and is, thus, a clear manifestation of releasing geometrical frustration of the kagome lattice. The smooth, linear enhancement of the transition temperature in Fig. 5(d) agrees with the unchanging AFM structure under strain, which we verified by magnetic field sweeps like in Fig. 3(b).

Let us assess the observed strain-tuning effects in the context of other materials where the structure impacts the magnetic properties. In $ZnCu_3(OH)_6Cl_2$, indications of Dzyaloshinskii–Moriya interaction [21,25] and even symmetry breaking [55] have been reported, likely related to magnetoelastic coupling [56], while hydrostatic pressure yields an emergence of magnetic order [57]. The compound studied here shows structural similarities to the "pinwheel" kagome structure of $Rb_2Cu_3SnF_{12}$ [42,58] and a barlowite polymorph [43]. To that end, Y-kapellasite is frustrated in a

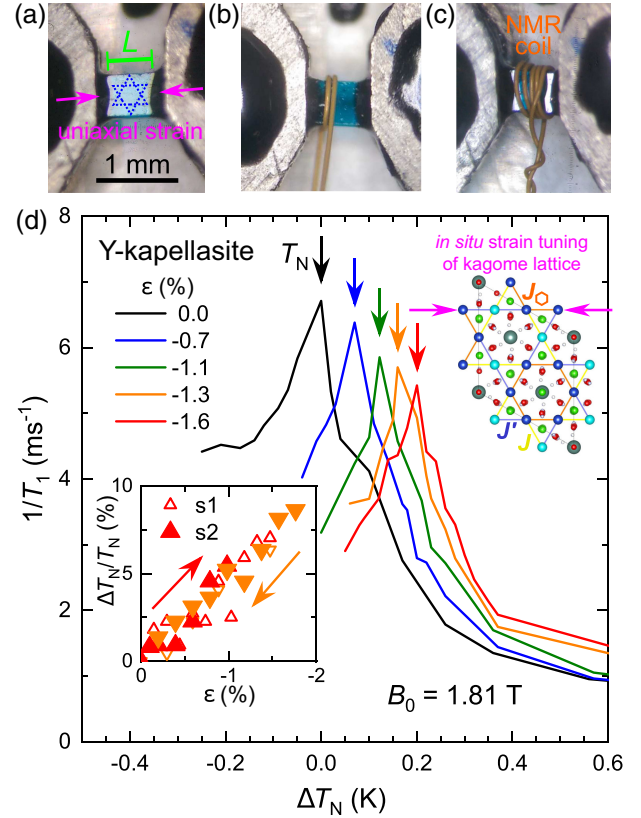FIG. 5. *In situ* strain tuning of frustrated magnetism in $Y_3Cu_9(OH)_{19}Cl_8$. (a)–(c) For NMR experiments under uniaxial strain a single crystal was glued between the two arms of a piezoelectric strain cell (a), and, subsequently, an NMR coil was wound around it (b),(c). (d) T_1^{-1} was measured for $B \| a$ upon uniaxial compression of the kagome lattice parallel to the Cu^{2+} chains (sketched on the top right; cf. Fig. 1). Inset: in-plane strain $\varepsilon = -1.6\%$ [44] results in a considerable enhancement of the transition temperature by $\Delta T_N / T_N \approx 10\%$.

different way than herbertsmithite or kapellasite, which both exhibit an undistorted kagome lattice—at the expense of severe Zn/Cu antisite disorder [6], that is also relevant in Zn-barlowite [13,43]. A clear indication for a structural involvement in the magnetic degrees of freedom is the recently discovered structural anomaly at 32 K [31]—only below this temperature does the relaxation rate soar well above ^{1}H T_1^{-1} of $ZnCu_3(OH)_6Cl_2$ (pink dotted line in Fig. 4 from Ref. [51]) that is of similar magnitude at higher T. It is tempting to link the 32 K anomaly in Y-kapellasite with the recent observation of spin singlets setting in at a similar temperature in herbertsmithite and barlowite [27], nourishing the idea that this is a ubiquitous magnetostructural instability of copper hydroxide kagome systems. While Cu/Zn disorder in the latter two compounds may conceal associated structural fingerprints around 30 K, lattice effects were found already at higher temperatures [24,25,51,59]. Depending on the particular deviations from a perfect kagome lattice in the different materials, such as

inequivalent lattice sites or disorder, the anomaly may manifest in various forms, e.g., leading to dimerization or other patterns. An intriguing scenario could be that this is the onset of nematic order below a crossover temperature $T^\star \gg T_N$ predicted for a distorted kagome lattice [52]. Extending our present strain-tuning experiments on Y-kapellasite to higher temperatures would enable direct scrutiny of this issue and, thus, remains a *desideratum* for future work.

In conclusion, we performed comprehensive ^{1}H NMR investigations on $Y_3Cu_9(OH)_{19}Cl_8$ as a function of temperature, magnetic field, and uniaxial strain. Under unstrained conditions, we find spectral evidence for unusual AFM order of $\vec{Q} = (1/3 \times 1/3)$ type [33] in this distorted kagome compound, with an order parameter growing in a mean-field fashion below $T_N = 2.2$ K. Clear signatures for AFM are also seen in the linewidth and spin-lattice relaxation rate, which are dominated by proton dynamics at elevated temperatures while magnetic correlations become dominant below the structural anomaly at 32 K [31]. Based on this characterization at ambient pressure, we applied *in situ* uniaxial stress parallel to the kagome layers yielding a linear increase of T_N with strain, in accord with theoretical predictions [52]. Through realizing for the first time a controlled release of frustration—*in situ* within one single crystal—our findings evidence its crucial importance for correlated quantum magnets and spin liquids, opening the door for similar studies in triangular, honeycomb, and other kagome systems. The pioneering strain-tuning approach presented here is ideally suited to resolve the magnetic ground states of existing materials and to discover novel exotic spin phases beyond state-of-the-art theoretical frameworks [2,4,33].

---

[*]pustogow@ifp.tuwien.ac.at

[1] L. Balents, Spin liquids in frustrated magnets, Nature (London) **464**, 199 (2010).

[2] L. Savary and L. Balents, Quantum spin liquids: A review, Rep. Prog. Phys. **80**, 016502 (2017).

[3] Y. Zhou, K. Kanoda, and T.-K. Ng, Quantum spin liquid states, Rev. Mod. Phys. **89**, 025003 (2017).

[4] C. Broholm, R. J. Cava, S. A. Kivelson, D. G. Nocera, M. R. Norman, and T. Senthil, Quantum spin liquids, Science **367**, eaay0668 (2020).

[5] A. Olariu, P. Mendels, F. Bert, F. Duc, J. C. Trombe, M. A. de Vries, and A. Harrison, ^{17}O NMR study of the intrinsic magnetic susceptibility and spin dynamics of the quantum kagome antiferromagnet $ZnCu_3(OH)_6Cl_2$, Phys. Rev. Lett. **100**, 087202 (2008).

[6] D. E. Freedman, T. H. Han, A. Prodi, P. Müller, Q.-Z. Huang, Y.-S. Chen, S. M. Webb, Y. S. Lee, T. M. McQueen, and D. G. Nocera, Site specific x-ray anomalous dispersion of the geometrically frustrated Kagomé magnet, herbertsmithite, $ZnCu_3(OH)_6Cl_2$, J. Am. Chem. Soc. **132**, 16185 (2010).

[7] I. Kimchi, A. Nahum, and T. Senthil, Valence bonds in random quantum magnets: Theory and application to YbMgGaO$_4$, Phys. Rev. X **8**, 031028 (2018).

[8] K. Riedl, R. Valentí, and S. M. Winter, Critical spin liquid versus valence-bond glass in a triangular-lattice organic antiferromagnet, Nat. Commun. **10**, 2561 (2019).

[9] A. Pustogow, T. Le, H.-H. Wang, Y. Luo, E. Gati, H. Schubert, M. Lang, and S. E. Brown, Impurity moments conceal low-energy relaxation of quantum spin liquids, Phys. Rev. B **101**, 140401(R) (2020).

[10] R. W. Smaha, I. Boukahil, C. J. Titus, J. M. Jiang, J. P. Sheckelton, W. He, J. Wen, J. Vinson, S. G. Wang, Y.-S. Chen, S. J. Teat, T. P. Devereaux, C. Das Pemmaraju, and Y. S. Lee, Site-specific structure at multiple length scales in kagome quantum spin liquid candidates, Phys. Rev. Mater. **4**, 124406 (2020).

[11] B. Miksch, A. Pustogow, M. Javaheri Rahim, A. A. Bardin, K. Kanoda, J. A. Schlueter, R. Hübner, M. Scheffler, and M. Dressel, Gapped magnetic ground state in quantum spin liquid candidate κ-$(BEDT-TTF)_2Cu_2(CN)_3$, Science **372**, 276 LP (2021).

[12] A. Pustogow, Thirty-year anniversary of κ-$(BEDT-TTF)_2Cu_2(CN)_3$: Reconciling the spin gap in a spin-liquid candidate, Solids **3**, 93 (2022).

[13] W. Yuan, J. Wang, P. M. Singer, R. W. Smaha, J. Wen, Y. S. Lee, and T. Imai, Emergence of the spin polarized domains in the kagome lattice Heisenberg antiferromagnet Zn-barlowite $(Zn_{0.95}Cu_{0.05})Cu_3(OD)_6FBr$, npj Quantum Mater. **7**, 120 (2022).

[14] Y. Li, D. Adroja, R. I. Bewley, D. Voneshen, A. A. Tsirlin, P. Gegenwart, and Q. Zhang, Crystalline electric-field randomness in the triangular lattice spin-liquid YbMgGaO$_4$, Phys. Rev. Lett. **118**, 107202 (2017).

[15] Y. Shimizu, K. Miyagawa, K. Kanoda, M. Maesato, and G. Saito, Spin liquid state in an organic mott insulator with a triangular lattice, Phys. Rev. Lett. **91**, 107001 (2003).

[16] T. Isono, H. Kamo, A. Ueda, K. Takahashi, M. Kimata, H. Tajima, S. Tsuchiya, T. Terashima, S. Uji, and H. Mori, Gapless quantum spin liquid in an organic spin-1/2 triangular-lattice κ-$H_3(Cat-EDT-TTF)_2$, Phys. Rev. Lett. **112**, 177201 (2014).

[17] Y. Shimizu, T. Hiramatsu, M. Maesato, A. Otsuka, H. Yamochi, A. Ono, M. Itoh, M. Yoshida, M. Takigawa, Y. Yoshida, and G. Saito, Pressure-tuned exchange coupling of a quantum spin liquid in the molecular triangular lattice $\kappa - (ET)_2Ag_2(CN)_3$, Phys. Rev. Lett. **117**, 107203 (2016).

[18] T. Itou, A. Oyamada, S. Maegawa, and R. Kato, Instability of a quantum spin liquid in an organic triangular-lattice antiferromagnet, Nat. Phys. **6**, 673 (2010).

[19] H. Takagi, T. Takayama, G. Jackeli, G. Khaliullin, and S. E. Nagler, Concept and realization of Kitaev quantum spin liquids, Nat. Rev. Phys. **1,** 264 (2019).

[20] P. Puphal, K. M. Zoch, J. Désor, M. Bolte, and C. Krellner, Kagome quantum spin systems in the atacamite family, Phys. Rev. Mater. **2,** 063402 (2018).

[21] M. R. Norman, *Colloquium:* Herbertsmithite and the search for the quantum spin liquid, Rev. Mod. Phys. **88,** 041002 (2016).

[22] M. P. Shores, E. A. Nytko, B. M. Bartlett, and D. G. Nocera, A structurally perfect $S = (1/2)$ kagomé antiferromagnet, J. Am. Chem. Soc. **127,** 13462 (2005).

[23] T.-H. Han, J. S. Helton, S. Chu, D. G. Nocera, J. A. Rodriguez-Rivera, C. Broholm, and Y. S. Lee, Fractionalized excitations in the spin-liquid state of a kagome-lattice antiferromagnet, Nature (London) **492,** 406 (2012).

[24] M. Fu, T. Imai, T.-H. Han, and Y. S. Lee, Evidence for a gapped spin-liquid ground state in a kagome Heisenberg antiferromagnet, Science **350,** 655 (2015).

[25] A. Zorko, M. Herak, M. Gomilšek, J. van Tol, M. Velázquez, P. Khuntia, F. Bert, and P. Mendels, Symmetry reduction in the quantum kagome antiferromagnet herbertsmithite, Phys. Rev. Lett. **118,** 017202 (2017).

[26] P. Khuntia, M. Velazquez, Q. Barthélemy, F. Bert, E. Kermarrec, A. Legros, B. Bernu, L. Messio, A. Zorko, and P. Mendels, Gapless ground state in the archetypal quantum kagome antiferromagnet $ZnCu_3(OH)_6Cl_2$, Nat. Phys. **16,** 469 (2020).

[27] J. Wang, W. Yuan, P. M. Singer, R. W. Smaha, W. He, J. Wen, Y. S. Lee, and T. Imai, Emergence of spin singlets with inhomogeneous gaps in the kagome lattice Heisenberg antiferromagnets Zn-barlowite and herbertsmithite, Nat. Phys. **17,** 1109 (2021).

[28] I. I. Mazin, H. O. Jeschke, F. Lechermann, H. Lee, M. Fink, R. Thomale, and R. Valentí, Theoretical prediction of a strongly correlated Dirac metal, Nat. Commun. **5,** 4261 (2014).

[29] P. Puphal, K. M. Ranjith, A. Pustogow, M. Müller, A. Rogalev, K. Kummer, J.-C. Orain, C. Baines, M. Baenitz, M. Dressel, E. Kermarrec, F. Bert, P. Mendels, and C. Krellner, Tuning of a kagome magnet: Insulating ground state in Ga-substituted $Cu_4(OH)_6Cl_2$, Phys. Status Solidi B **256,** 1800663 (2019).

[30] P. Puphal, M. Bolte, D. Sheptyakov, A. Pustogow, K. Kliemt, M. Dressel, M. Baenitz, and C. Krellner, Strong magnetic frustration in $Y_3Cu_9(OH)_{19}Cl_8$: A distorted kagome antiferromagnet, J. Mater. Chem. C **5,** 2629 (2017).

[31] D. Chatterjee, P. Puphal, Q. Barthélemy, J. Willwater, S. Süllow, C. Baines, S. Petit, E. Ressouche, J. Ollivier, K. M. Zoch, C. Krellner, M. Parzer, A. Riss, F. Garmroudi, A. Pustogow, P. Mendels, E. Kermarrec, and F. Bert, From spin liquid to magnetic ordering in the anisotropic kagome Y-kapellasite $Y_3Cu_9(OH)_{19}Cl_8$: A single-crystal study, Phys. Rev. B **107,** 125156 (2023).

[32] W. Sun, Y.-X. Huang, S. Nokhrin, Y. Pan, J.-X. Mi, P. Mendels, A. S. Wills, J. X. Mi, A. Amato, J. van Tol, A. Ozarowski, A. S. Wills, P. Mendels, and A. S. Wills, Perfect Kagomé lattices in $YCu_3(OH)_6Cl_3$: A new candidate for the quantum spin liquid state, J. Mater. Chem. C **4,** 8772 (2016).

[33] M. Hering, F. Ferrari, A. Razpopov, I. I. Mazin, R. Valentí, H. O. Jeschke, and J. Reuther, Phase diagram of a distorted kagome antiferromagnet and application to Y-kapellasite, npj Comput. Mater. **8,** 10 (2022).

[34] C. W. Hicks, M. E. Barber, S. D. Edkins, D. O. Brodsky, and A. P. Mackenzie, Piezoelectric-based apparatus for strain tuning, Rev. Sci. Instrum. **85,** 65003 (2014).

[35] A. Pustogow, Y. Li, I. Voloshenko, P. Puphal, C. Krellner, I. I. Mazin, M. Dressel, and R. Valentí, Nature of optical excitations in the frustrated kagome compound herbertsmithite, Phys. Rev. B **96,** 241114(R) (2017).

[36] Q. Barthélemy, P. Puphal, K. M. Zoch, C. Krellner, H. Luetkens, C. Baines, D. Sheptyakov, E. Kermarrec, P. Mendels, and F. Bert, Local study of the insulating quantum kagome antiferromagnets $YCu_3(OH)_6O_xCl_{3-x}(x = 0, 1/3)$, Phys. Rev. Mater. **3,** 074401 (2019).

[37] T. Biesner, S. Roh, A. Razpopov, J. Willwater, S. Süllow, Y. Li, K. M. Zoch, M. Medarde, J. Nuss, D. Gorbunov, Y. Skourski, A. Pustogow, S. E. Brown, C. Krellner, R. Valentí, P. Puphal, and M. Dressel, Multi-center magnon excitations open the entire Brillouin zone to terahertz magnetometry of quantum magnets, Adv. Quantum Technol. **2022,** 2200023 (2022).

[38] A. Zorko, M. Pregelj, M. Klanjšek, M. Gomilšek, Z. Jagličić, J. S. Lord, J. A. T. Verezhak, T. Shang, W. Sun, and J.-X. Mi, Coexistence of magnetic order and persistent spin dynamics in a quantum kagome antiferromagnet with no intersite mixing, Phys. Rev. B **99,** 214441 (2019).

[39] H. Ishikawa, M. Yoshida, K. Nawa, M. Jeong, S. Krämer, M. Horvatić, C. Berthier, M. Takigawa, M. Akaki, A. Miyake, M. Tokunaga, K. Kindo, J. Yamaura, Y. Okamoto, and Z. Hiroi, One-third magnetization plateau with a preceding novel phase in volborthite, Phys. Rev. Lett. **114,** 227202 (2015).

[40] D. Boldrin and A. S. Wills, $SrCu_3V_2O_8(OH)_2$—dynamic Jahn–Teller distortions and orbital frustration in a new $S =$ kagome antiferromagnet, J. Mater. Chem. C **3,** 4308 (2015).

[41] S. Spachmann, P. Berdonosov, M. Markina, A. Vasiliev, and R. Klingeler, Linear magnetoelastic coupling and magnetic phase diagrams of the Buckled-Kagomé antiferromagnet $Cu_3Bi(SeO_3)_2O_2C$, Sci. Rep. **12,** 7383 (2022).

[42] K. Matan, T. Ono, Y. Fukumoto, T. J. Sato, J. Yamaura, M. Yano, K. Morita, and H. Tanaka, Pinwheel valence-bond solid and triplet excitations in the two-dimensional deformed kagome lattice, Nat. Phys. **6,** 865 (2010).

[43] R. W. Smaha, W. He, J. M. Jiang, J. Wen, Y.-F. Jiang, J. P. Sheckelton, C. J. Titus, S. G. Wang, Y.-S. Chen, S. J. Teat, A. A. Aczel, Y. Zhao, G. Xu, J. W. Lynn, H.-C. Jiang, and Y. S. Lee, Materializing rival ground states in the barlowite family of kagome magnets: Quantum spin liquid, spin ordered, and valence bond crystal states, npj Quantum Mater. **5,** 23 (2020).

[44] See Supplemental Material at http://link.aps.org/supplemental/10.1103/PhysRevLett.131.256501 for details on (I) NMR experiments, (II) simulation of NMR spectra, and (III) uniaxial-strain experiments, which includes Refs. [30,31,34,37,45–50].

[45] Y. Luo, A. Pustogow, P. Guzman, A. P. Dioguardi, S. M. Thomas, F. Ronning, N. Kikugawa, D. A. Sokolov, F. Jerzembeck, A. P. Mackenzie, C. W. Hicks, E. D. Bauer,

I. I. Mazin, and S. E. Brown, Normal state ^{17}O NMR studies of Sr_2RuO_4 under uniaxial stress, Phys. Rev. X **9,** 021044 (2019).

[46] A. Pustogow, Y. Luo, A. Chronister, Y.-S. Su, D. A. Sokolov, F. Jerzembeck, A. P. Mackenzie, C. W. Hicks, N. Kikugawa, S. Raghu, E. D. Bauer, and S. E. Brown, Constraints on the superconducting order parameter in Sr2RuO4 from oxygen-17 nuclear magnetic resonance, Nature (London) **574,** 72 (2019).

[47] A. Chronister, M. Zingl, A. Pustogow, Y. Luo, D. A. Sokolov, F. Jerzembeck, N. Kikugawa, C. W. Hicks, J. Mravlje, E. D. Bauer, J. D. Thompson, A. P. Mackenzie, A. Georges, and S. E. Brown, Tuning the Fermi liquid crossover in Sr_2RuO_4 with uniaxial stress, npj Quantum Mater. **7,** 113 (2022).

[48] A. Steppke, L. Zhao, M. E. Barber, T. Scaffidi, F. Jerzembeck, H. Rosner, A. S. Gibbs, Y. Maeno, S. H. Simon, A. P. Mackenzie, and C. W. Hicks, Strong peak in T_c of Sr_2RuO_4 under uniaxial pressure, Science **355,** eaaf9398 (2017).

[49] M. E. Barber, A. Steppke, A. P. Mackenzie, and C. W. Hicks, Piezoelectric-based uniaxial pressure cell with integrated force and displacement sensors, Rev. Sci. Instrum. **90,** 23904 (2019).

[50] M. E. Barber, F. Lechermann, S. V. Streltsov, S. L. Skornyakov, S. Ghosh, B. J. Ramshaw, N. Kikugawa, D. A. Sokolov, A. P. Mackenzie, C. W. Hicks, and I. I. Mazin, Role of correlations in determining the Van Hove strain in Sr_2RuO_4, Phys. Rev. B **100,** 245139 (2019).

[51] T. Imai, E. A. Nytko, B. M. Bartlett, M. P. Shores, and D. G. Nocera, ^{63}Cu, ^{35}Cl, and ^1H NMR in the $S = \frac{1}{2}$ kagome lattice $ZnCu_3(OH)_6Cl_2$, Phys. Rev. Lett. **100,** 077203 (2008).

[52] H. Masuda, T. Okubo, and H. Kawamura, Finite-temperature transition of the antiferromagnetic Heisenberg model on a distorted kagome lattice, Phys. Rev. Lett. **109,** 057201 (2012).

[53] We expect that the maximal compression of the sample is somewhat lower (closer to $\varepsilon \approx 1\%$) than the present estimate ($\varepsilon \approx 1.6\%$) using the built-in capacitive sensor, as elaborated at the end of Sec. III in Supplemental Material [44].

[54] A notable exception is Sr_2RuO_4, where the length changes upon uniaxial strain do not involve a change of bond angles [45–48].

[55] M. R. Norman, N. J. Laurita, and D. Hsieh, Valence bond phases of herbertsmithite and related copper kagome materials, Phys. Rev. Res. **2,** 013055 (2020).

[56] Y. Li, A. Pustogow, M. Bories, P. Puphal, C. Krellner, M. Dressel, and R. Valentí, Lattice dynamics in the spin-$\frac{1}{2}$ frustrated kagome compound herbertsmithite, Phys. Rev. B **101,** 161115(R) (2020).

[57] D. P. Kozlenko, A. F. Kusmartseva, E. V. Lukin, D. A. Keen, W. G. Marshall, M. A. de Vries, and K. V. Kamenev, From quantum disorder to magnetic order in an $s = 1/2$ kagome lattice: A structural and magnetic study of herbertsmithite at high pressure, Phys. Rev. Lett. **108,** 187207 (2012).

[58] M. S. Grbić, S. Krämer, C. Berthier, F. Trousselet, O. Cépas, H. Tanaka, and M. Horvatić, Microscopic properties of the pinwheel kagome compound $Rb_2Cu_3SnF_{12}$, Phys. Rev. Lett. **110,** 247203 (2013).

[59] J. Wang, W. Yuan, P. M. Singer, R. W. Smaha, W. He, J. Wen, Y. S. Lee, and T. Imai, Freezing of the lattice in the kagome lattice Heisenberg antiferromagnet Zn-barlowite $ZnCu_3(OD)_6FBr$, Phys. Rev. Lett. **128,** 157202 (2022).